Article no. 46

THE CIVIL ENGINEERING JOURNAL 4-2018

NUMERICAL INVESTIGATION OF THE PERFORMANCE OF INSULATED FRP-STRENGTHENED REINFORCED CONCRETE BEAMS IN FIRE

Osama El-Mahdy[1], Gehan Hamdy[2] and Moustafa Abdullah[2]

1. *Department of Civil Engineering, Faculty of Engineering at Shoubra, Benha University, Shoubra, Cairo, Egypt; osama.alhenawy@feng.bu.edu.eg, os8294@hotmail.com*
2. *Department of Civil Engineering, Faculty of Engineering at Shoubra, Benha University, Shoubra, Cairo, Egypt*

ABSTRACT

Fiber reinforced polymers (FRP) have been widely used in retrofitting and strengthening of deteriorated or deficient reinforced concrete (RC) elements. A major concern about those systems is their performance under elevated temperature which limits the application of FRP for strengthening requirements. Fire protection of the strengthening FRP system can be made by applying an external coating layer of a thermal resisting material. In order to predict the fire performance of such insulated FRP-strengthened members and their efficiency, experimental investigations are required to be carried out for such elements under realistic fire conditions, which requires time and cost.

This paper presents numerical modelling of RC beams strengthened with externally bonded FRP and insulated by a fire protection layer under elevated temperature specified by standard fire tests. The nonlinear time domain transient thermal-stress finite element analysis is performed using the general purpose software ANSYS 12.1 in order to study the heat transfer mechanism and deformation within the beam for fire conditions initiating at the bottom side of the beam. The finite element model accounts for the variation in thermal and mechanical parameters of the constituent materials such as concrete, steel reinforcement bars, FRP and insulation material with temperature. Application is made on an FRP-strengthened and insulated RC T-beam which has been experimentally tested in the published literature in order to verify the adopted modelling procedure. The obtained numerical results are in good agreement with the experimental results regarding the temperature distribution across the beam and mid-span deflection. The presented procedure thus provides an economical and effective tool to investigate the effectiveness of fire insulation layers when subjected to high temperatures and to design thermal protection layers for FRP strengthening systems that satisfy fire resistance requirements specified in building codes and standards.

KEYWORDS

Fiber reinforced polymers, Flexural strengthening, Elevated temperature, Fire, Thermal insulation, Finite element, Nonlinear analysis

INTRODUCTION

Fiber reinforced polymers (FRP) have been used for retrofitting and strengthening of deteriorated concrete structures due to their advantageous properties such as light weight, corrosion resistance and high strength. Externally bonded FRP sheets or laminates have been demonstrated to successfully enhance the flexural and shear capacity of reinforced concrete (RC) beams [1]. However, there are increasing concerns about their performance in the case of fire. Polymer materials undergo change in mechanical properties and loss of stiffness and bond strength when exposed to temperatures higher than the glass transition temperature (T_g) which is about 60 – 82 °C for the common polymers and adhesives [2]. When the temperature rises to this level, such as likely to happen in the case of fire, damage will occur to the bond between the FRP and the concrete surface and consequently the effectiveness of the FRP strengthening is severely threatened and may be totally lost [2, 3]. Fire performance is pointed out as a critical factor that requires more research before FRP can be used with confidence in strengthening applications [2]. Specifications and design guidelines limit the use, increase the load factor or limit the desired strength enhancement in order to meet fire hazard [4, 5]. Higher values of strengthening limits are allowed only if it can be proved through testing and technical assessments that such fire protection systems can increase fire endurance of FRP systems to exceed the fire resistance rating of building codes [4, 5]. There are still no design guidelines available for FRP-reinforced or strengthened concrete structures under fire conditions regarded as one of the major threats to buildings and other structures.

Experimental studies were carried out for FPR-strengthened RC members under elevated temperatures or fire by several researchers [6- 10]. To provide protection of carbon fiber reinforced polymer (CFRP) from direct fire exposure, a coating layer of a thermal insulating material, typically gypsum products, was placed around the beam cross-section [11, 12]. A fire test program was conducted by Blontrock et al. [6] in which ten CFRP-strengthened RC beams protected with calcium silicate boards were subjected to the design service loads of Eurocode [13]. The best fire resistance was provided by fire insulation layer applied as U-shape over the bottom and sides of the beams [6]. Using a 50 mm thick layer of Perlite mortar has protected CFRP strengthening system against 500 °C for three hours with only 4 - 12% loss in its capacity [11]. Different coating layers of Perlite, Vermiculite and Portland Cement mortars in addition to clay and ceramic fiber were studied and experimentally demonstrated to give protection and maintain 90% of the residual flexural capacity of FRP-strengthened beams compared to control beams after a two-hour exposure to 600 °C [12].

Beam-slab assemblies strengthened with FRP laminates and protected with vermiculite-gypsum (VG) cementitious layer were tested by Williams et al. [14] by exposure to standard fire load of ASTM E119 [15]. Efficient thermal protection and three hours fire endurance ratings were achieved by a 25 mm and 38 mm thick layer of the VG insulation [14].

Some studies in the published literature addressed numerical modelling to predict the performance of FRP-strengthened RC members subjected to fire [16 - 18] and the heat transfer through the different insulation layers during fire exposure [19]. However, more research work is needed that addresses modelling the performance of FRP-strengthened structures under elevated temperatures, in order to enable analysts and designers to accurately predict the fire endurance and economically design thermal insulation layers for such structures.

OBJECTIVE

The present research aims at studying numerically the behaviour of RC beams strengthened by externally bonded FRP laminates and thermally protected, under standard fire test

loading, thereby providing an economic tool for design of fire protection for FRP-strengthened RC beams.

To achieve this aim, numerical modelling by finite elements is performed to represent the beam components and account for the variation in thermal and mechanical parameters of the different materials with temperature. Nonlinear time analysis is performed using ANSYS 12.1 [20] in order to study the heat transfer mechanism and deformations within the beam. The numerical results are presented and compared to the previously published experimental and numerical results [14, 19] in order to verify the efficiency of the adopted numerical procedure.

NUMERICAL MODELING AND ANALYSIS

Finite Element Modelling

Modelling is made by finite elements using ANSYS 12.1 [20] for a thermally protected CFRP-strengthened RC beam that has been subjected to fire test in the published literature [14]. The T-beam is simply supported with total length 4000 mm and clear span 3900 mm, has the cross-sectional dimensions of 400 mm depth, 1220 mm flange width, 150 mm flange thickness and 300 mm web thickness, as shown in Figure 1. The T-beam reinforcement details were as follows; the main steel reinforcement was two 20 mm diameter bars. Shear stirrups were 10 mm diameter bars spaced at 150 mm centre to centre. Concrete cover to the web stirrups was 40 mm and concrete cover for flange reinforcement was 25 mm. A CFRP laminate of 1.3 mm thick and 100 mm wide is adhered to the bottom of the beam along the span and stopped at 100 mm from the support. A layer of VG plaster having a thickness of 25 mm is applied on the beam soffit and web and extends for a distance of 125 mm underneath the flange, as shown in Figure 1, along the entire length of the beam.

The element types used for transient thermal and structural finite element analysis are listed in Table 1. Full bond is assumed between concrete and reinforcement bars, CFRP and insulation layer. The details of finite element model are shown in Figure 2.

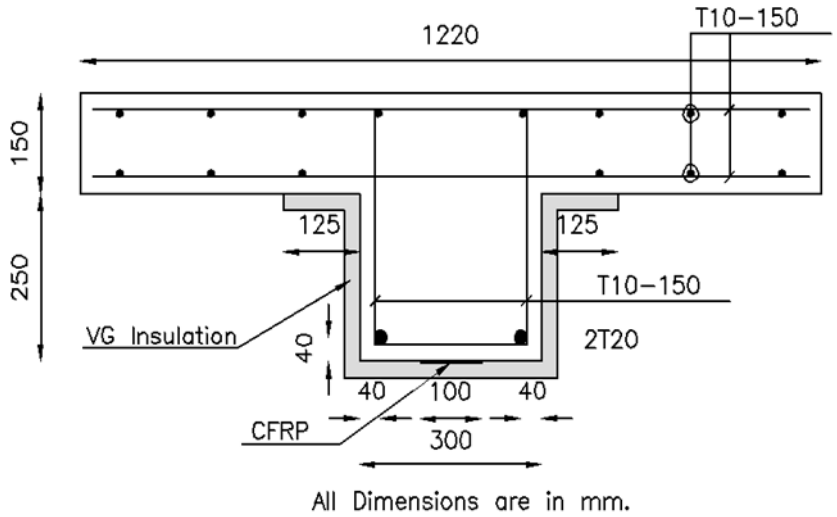

Fig. 1 - Experimentally tested T-beam cross-section [14]

Tab. 1 - Element types used for thermal and structural analyses

Material	Elements for thermal analysis	Elements for structural analysis
Concrete	SOLID70	SOLID65
Steel bars	LINK33	LINK8
CFRP layer	SHELL 57	SHELL 41
VG insulation	SOLID70	SOLID45

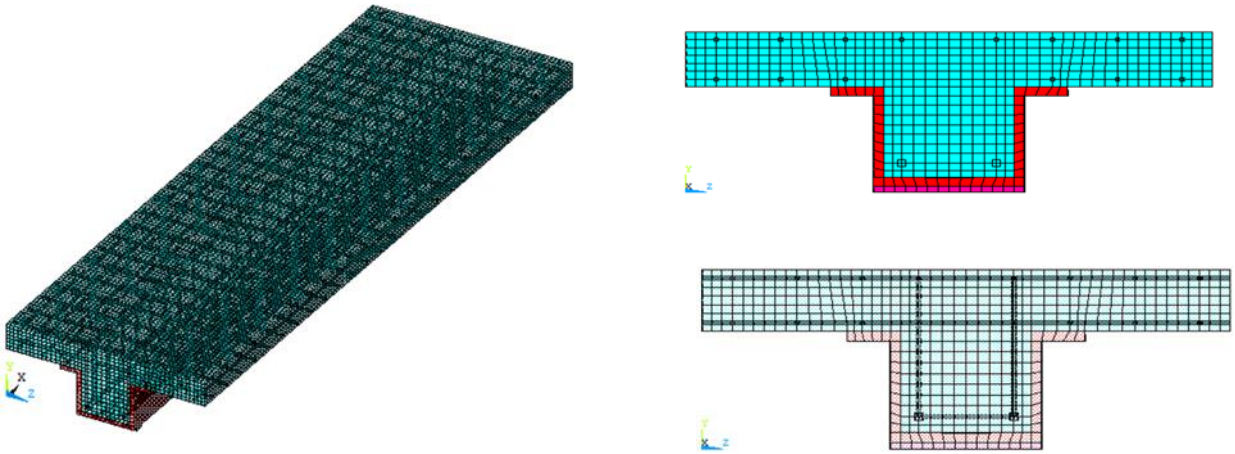

Fig. 2 - Finite Element Mesh of the Studied T-Beam

Material Mechanical and Thermal Properties

The concrete characteristic compressive strength is 41 MPa. The main steel reinforcement has yield and ultimate strengths of 500 and 650 MPa, respectively. The 10mm diameter reinforcement bars of stirrups and slab reinforcement have yield and ultimate strengths of 429 and 611 MPa, respectively. The 1.3 mm-thick CFRP laminate possesses a design tensile strength of 460 MPa in the direction of the fibres and ultimate elongation of 2.2% at failure [14]. Table 2 gives the values for the mechanical and thermal properties for concrete, steel reinforcement, CFRP and insulation materials at room temperature [19, 21].

Tab. 2 - Mechanical and thermal material properties at room temperature [19, 21]

Material	E_o MPa	K_o W/mm.K	C_o J/kg.K	μ	α	ρ_o Kg/m^3
Concrete	30200	2.7×10^{-3}	722.8	0.20	6.08×10^{-6}	2400
Steel bars	210000	5.2×10^{-2}	452.2	0.30	6.00×10^{-6}	7860
CFRP	228000	1.3×10^{-3}	1310	0.28	-0.90×10^{-6}	1600
VG Insulation	2100	2.5×10^{-4}	1654	0.30	1.70×10^{-5}	269

Note: E_o *:* stiffness modulus, K_o : thermal conductivity, C_o *:* specific heat, ρ_o : material density, α *:* coefficient of thermal expansion, and μ *:* Poisson's ratio.

The thermal and mechanical properties at elevated temperature for concrete and steel are available in the literature and the main equations are mentioned herein [13, 21, 22]. The steel reinforcement density is considered by Eurocode [22] to remain constant under elevated temperature. Density of concrete changes due to elevated temperature according to Equation. (1):

$$\rho(T) = \rho\ (20^oC) \qquad \text{for} \quad 20^oC \le T \le 115^oC \qquad (1.a)$$

$$\rho(T) = \rho\ (20^oC)\left(1 - \frac{0.02(T-115)}{85}\right) \qquad \text{for} \quad 115^oC < T \le 200^oC \qquad (1.b)$$

$$\rho(T) = \rho\ (20^oC)\left(0.98 - \frac{0.03(T-200)}{200}\right) \quad \text{for} \quad 200^oC < T \leq 400^oC \quad (1.c)$$

$$\rho(T) = \rho\ (20^oC)\left(0.95 - \frac{0.07(T-400)}{800}\right) \quad \text{for} \quad 400^oC < T \leq 1200^oC \quad (1.d)$$

Thermal conductivity of concrete changes with temperature according to Equation (2) and the variation in thermal conductivity of steel reinforcement with temperature is given in Equations. (3).

$$K(T) = 2 - 0.2451\left(\frac{T}{100}\right) + 0.0107\left(\frac{T}{100}\right)^2 \quad in\ \left(\frac{W}{m}.K\right) \quad \text{for} \quad 20^oC \leq T \leq 1200^oC \quad (2)$$

$$K(T) = 54 - 3.33x10^{-2} \quad in\ \left(\frac{W}{m}.K\right) \quad \text{for} \quad 20^oC \leq T \leq 800^oC \quad (3.a)$$

$$K(T) = 27.30 \quad in\ \left(\frac{W}{m}.K\right) \quad \text{for} \quad 800^oC < T \leq 1200^oC \quad (3.b)$$

The specific heat of concrete changes with temperature according to Equations. (4). The peak specific heat of concrete depends mainly on the moisture content and occurs between 100°C and 115°C with linear decrease between 115°C and 200°C. For zero moisture content the peak specific heat is 900 J/kg K, while for moisture content 1.5 % and 3% of concrete weight the peak specific heat is 1470 J/kg K and 2020 J/kg K, respectively. For the beam of the present study, moisture content equal to 3 % of concrete weight is adopted throughout the modelling.

$$C(T) = 900 \quad in\ \left(\frac{J}{Kg}.K\right) \quad \text{for} \quad 20^oC \leq T \leq 100^oC \quad (4.a)$$

$$C(T) = 900 + (T - 100) \quad in\ \left(\frac{J}{Kg}.K\right) \quad \text{for} \quad 100^oC < T \leq 200^oC \quad (4.b)$$

$$C(T) = 1000 + \frac{(T-200)}{2} \quad in\ \left(\frac{J}{Kg}.K\right) \quad \text{for} \quad 200^oC < T \leq 400^oC \quad (4.c)$$

$$C(T) = 1100 \quad in\ \left(\frac{J}{Kg}.K\right) \quad \text{for} \quad 400^oC < T \leq 1200^oC \quad (4.d)$$

Equations (5) show the change in specific heat for steel reinforcement with temperature as given by Eurocode [22], for temperature range between 20 °C to 1200 °C.

$$C(T) = 425 + 7.73x10^{-1}\,T - 1.69x10^{-3}\,T^2 + 2.22x10^{-6}\,T^3 \quad in\ \left(\frac{J}{Kg}.K\right) \quad \text{for} \quad 20^oC \leq T \leq 600^oC \quad (5.a)$$

$$C(T) = 666 + \left(\frac{13002}{738 - T}\right) \quad in\ \left(\frac{J}{Kg}.K\right) \quad \text{for} \quad 600^oC < T \leq 735^oC \quad (5.b)$$

$$C(T) = 545 + \left(\frac{17820}{T - 731}\right) \quad in\ \left(\frac{J}{Kg}.K\right) \quad \text{for} \quad 735^oC \leq T < 900^oC \quad (5.c)$$

$$C(T) = 650 \quad in\ \left(\frac{J}{Kg}.K\right) \quad \text{for} \quad 900^oC \leq T \leq 1200^oC \quad (5.d)$$

The stress-strain curves for concrete in compression under elevated temperature adopted in the present study are shown in Figure 3 (a), and the variation of concrete tensile strength with temperature is shown in Figure 3 (b) [14, 21]. The variation of the mechanical and the thermal properties of FRP and the materials used for thermal insulation is addressed in researches and not quite established. In this study, the thermal and mechanical properties of CFRP and VG insulation and their variation with temperature are based on the findings of other researchers [23 - 25].

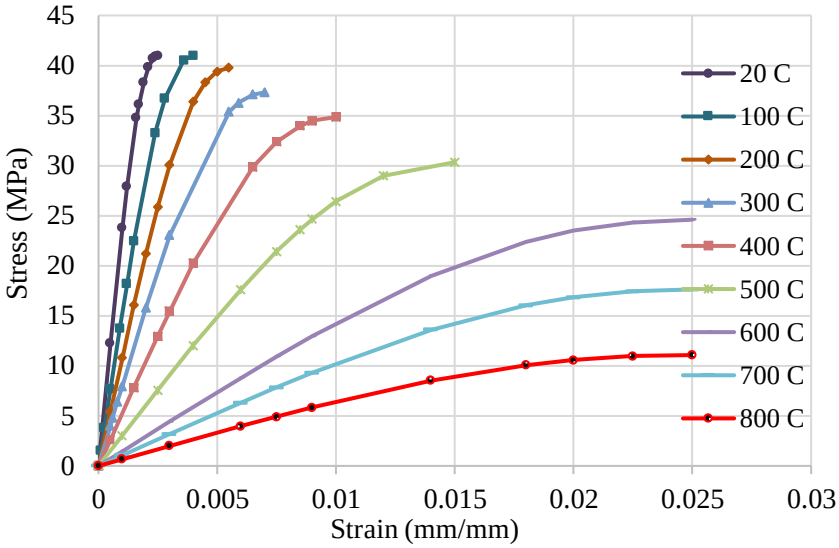

(a) Stress-strain curves in compression under elevated temperature

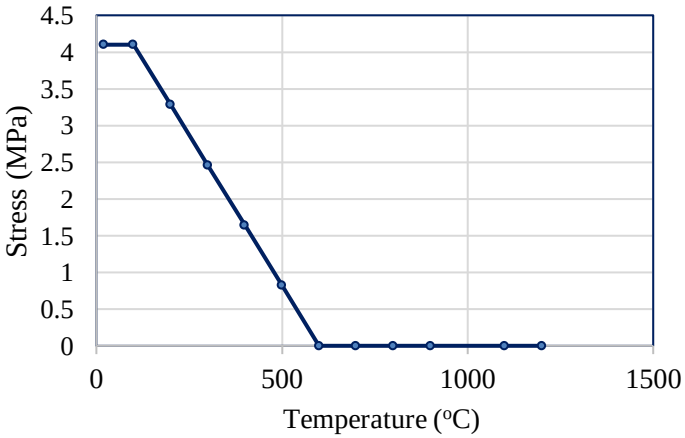

(b) Variation of concrete tensile strength with temperature

Fig. 3 - Concrete mechanical behaviour under elevated temperature

Nonlinear Analysis Parameters, Loading and Boundary Conditions

Concrete is modelled using the standard nonlinear constitutive concrete material model implemented within ANSYS [20]. Based on the formulation by Williams and Warnke [26], a multi-nonlinear compressive stress-strain curve is pointed. When a crack occurs, elastic modulus of the concrete element is set to zero in the direction parallel to the principal tensile stress direction. Crushing occurs when all principal stresses are compressive and are outside the failure surface; then the elastic modulus is set to zero in all directions and the element local stiffness becomes zero causing large displacement and divergence in the solution.

The analysis is carried out as two consecutive load cases. First, in the transient thermal analysis load case, standard temperature-time conditions described by ASTM E119 [15] and shown in Figure 4 are applied as nodal temperature-versus-time to the bottom surface of the T-beam. Equation 6 gives the ASTM E119 time temperature loading applied to the studied beam.

$$T = 20 + 750\left(1 - e^{-0.49\sqrt{t}}\right) + 22\sqrt{t} \qquad (6)$$

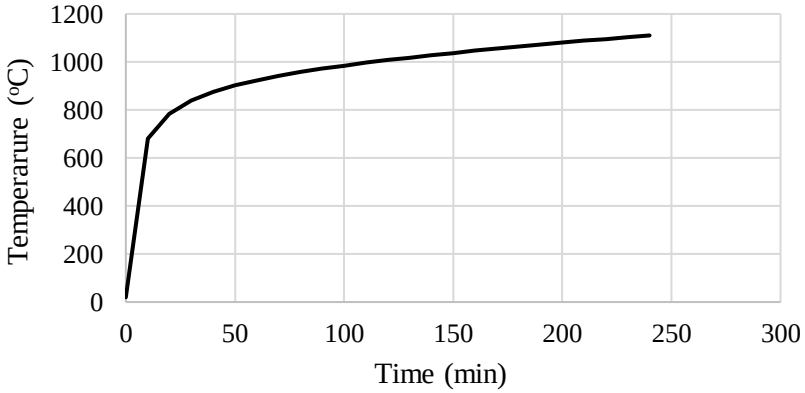

Fig. 4 - Applied temperature conforming to standard fire test curve of ASTM E119

The thermal gradient distribution in the T-beam obtained from the thermal analysis is next applied to the beam as nodal temperatures at several time load steps and sub-steps and structural stress analysis is performed. The experimentally applied sustained uniformly distributed load of 34 KN/m [14] is simulated by applying a pressure of 0.0278 MPa to the top surface of the T-beam flange.

NUMERICAL RESULTS AND DISCUSSION

In order to validate the accuracy of the model developed in this study, the obtained finite elements results are compared to the published experimental and numerical results. The thermal analyses results are evaluated by checking the temperatures at key locations with temperature gradients between the key locations of the beam model. The nodal temperature distribution within the T-beam cross section after one, three and four hours of fire exposure are shown in Figure 5.

The variation with time of the numerically calculated temperatures in VG, CFRP, and concrete at the same points that were measured in the experiment work [14] are plotted in Figure 6. It can be observed from Figure 6 that, there is a good agreement between the presented numerically predicted temperatures and the published experimental and numerical results [14, 19]. The average temperature of the steel reinforcement is less than 270 °C after four hours of fire exposure, which is below the ASTM E119 temperature limit of 593 °C.

Figure 7 shows the numerically predicted and the experimentally measured mid-span deflection at the centreline of the cross section throughout the fire exposure time. It is obvious that the mid-span deflection increases steadily during the fire exposure. The increase in deflection is associated with increase in the total strain on the beam tension side. This behaviour occurred as a result of rise of temperature of the CFRP and reinforcing steel on the tension side of the beam, thus reducing their stiffnesses, which caused further beam deflection. It is observed from Figure 7 that, the predicted mid-span deflection matches very closely the measured experimental one [14]. The deflection continues to increase nonlinearly in the numerical model under the sustained load.

The time until failure in both the finite element model and experiment is more than the fire endurance ratings required by North American standards in typical building applications. Furthermore, the accuracy of the adopted model herein is due to modelling the FRP system using shell elements rather than the solid elements used in the published model [19], in addition to proper description of the constituent materials properties and the refined meshing used in the present model.

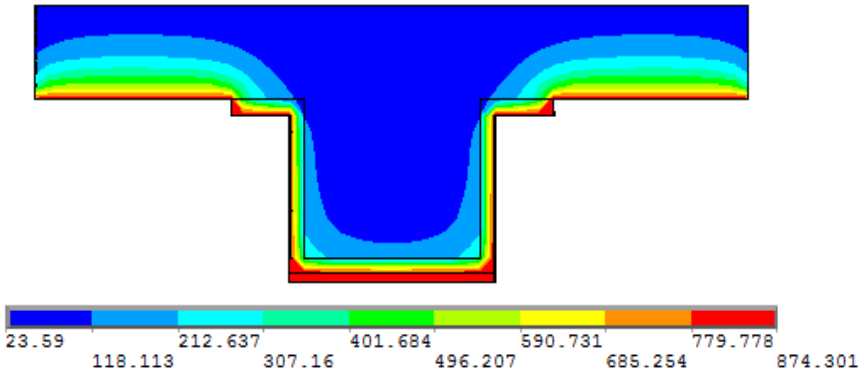

Temperatures (°C) after one hour

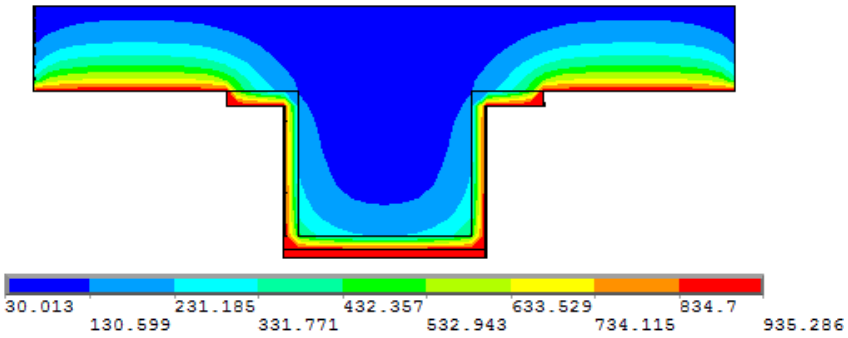

(a) Temperatures (°C) after three hours

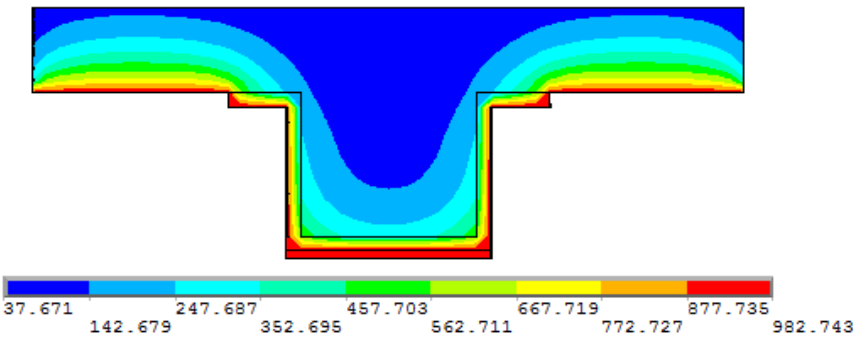

(b) Temperatures (°C) after four hours

Fig. 5 - Numerically predicted temperature distribution in the beam cross-section

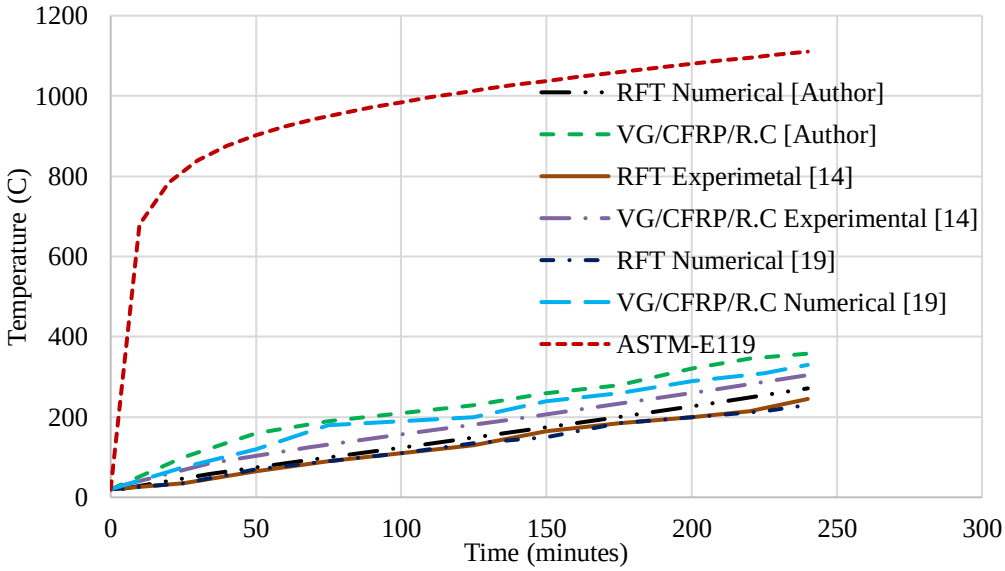

Fig. 6 - Numerical results of temperature versus time compared to experimental results

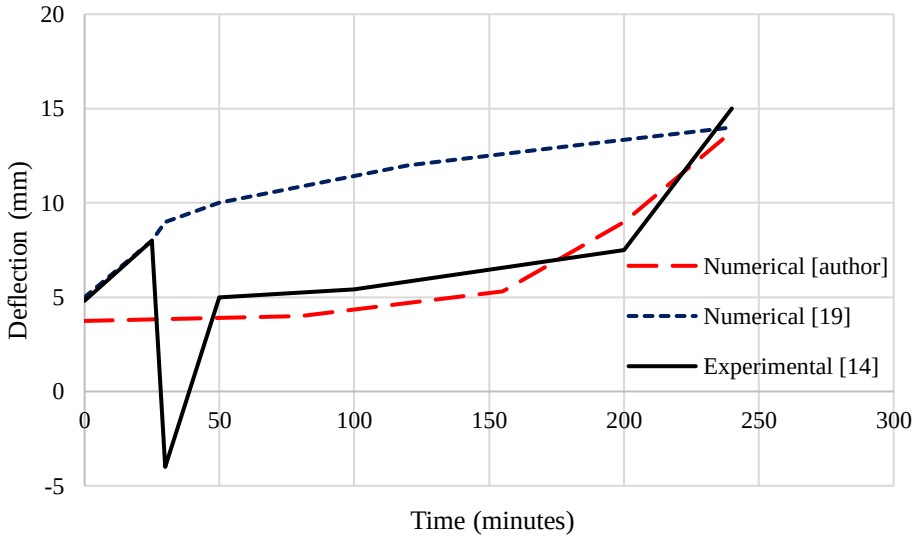

Fig. 7 - Variation of mid-span deflection with exposure time

Figure 8 shows the numerically predicated vertical deflection of the studied beam under elevated temperature after one, three and four hours of exposure to standard fire temperature. The mid-span deflection increases with time due to heating the bottom surface of the beam resulting in additional tensile strains which increase the mid-span deflection of the studied beam. Also, Figure 9 shows the numerically predicted cracks in the studied beam cross-section after one, three and four hours of exposure to elevated temperature. The number and width of cracks increases with exposure time due to the increase in the total strain in concrete resulting from both structural and thermal loading conditions Figure 10 shows the 3-D developed crack patterns after four hours. Again. the comparison of crack patterns held between the model results with the experimental work results presented in this paper, shows a good correlation achievement between the numerical and experimental results.

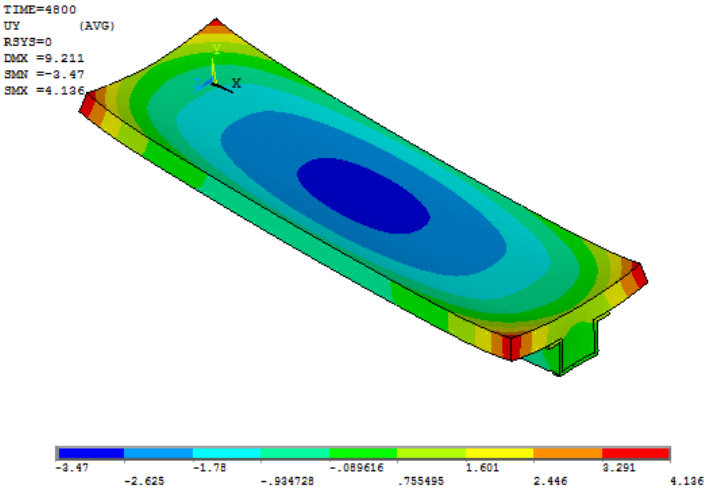

(a) Deflection (mm) after one hour

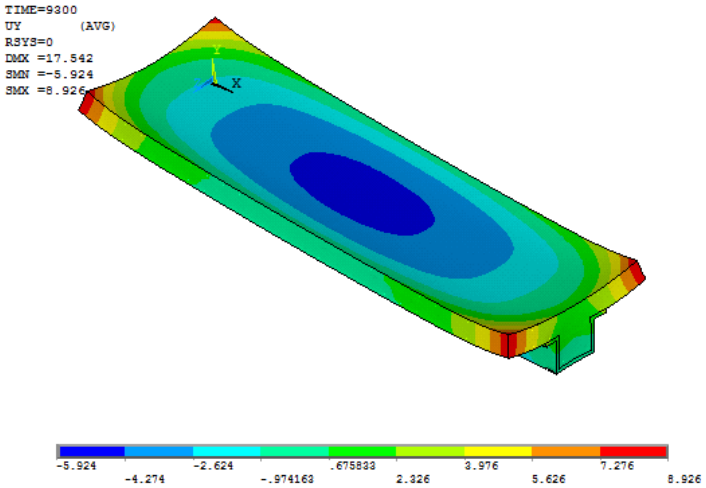

(b) Deflection (mm) after three hours

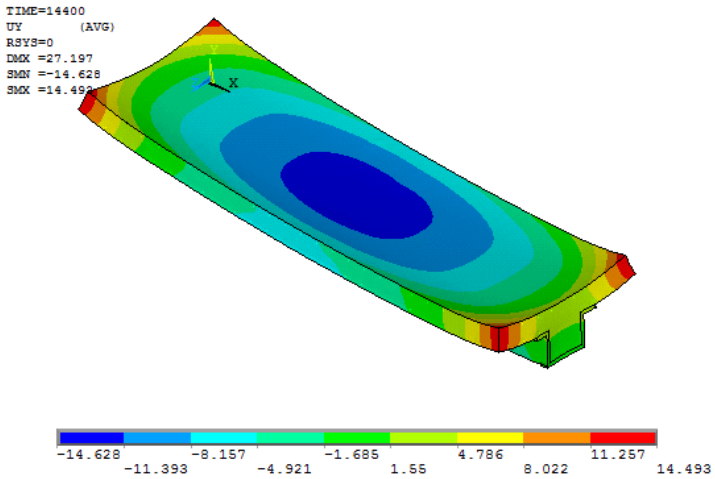

(c) Deflection (mm) after four hours

Fig. 8 - Numerically evaluated deflections after exposure to elevated temperature

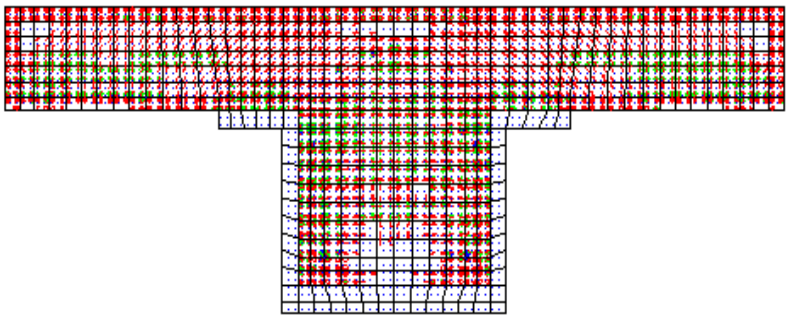

(a) Cracking after one hour

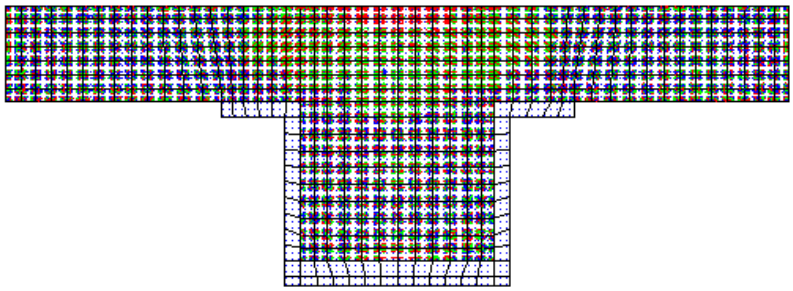

(b) Cracking after three hours

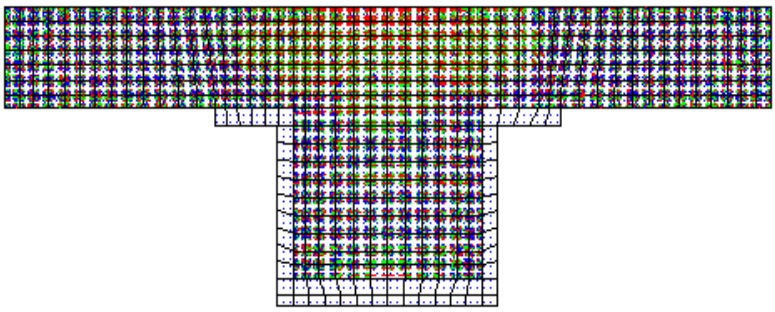

(c) Cracking after four hours

Fig. 9 - Numerical results of the cracks in the beam cross-section

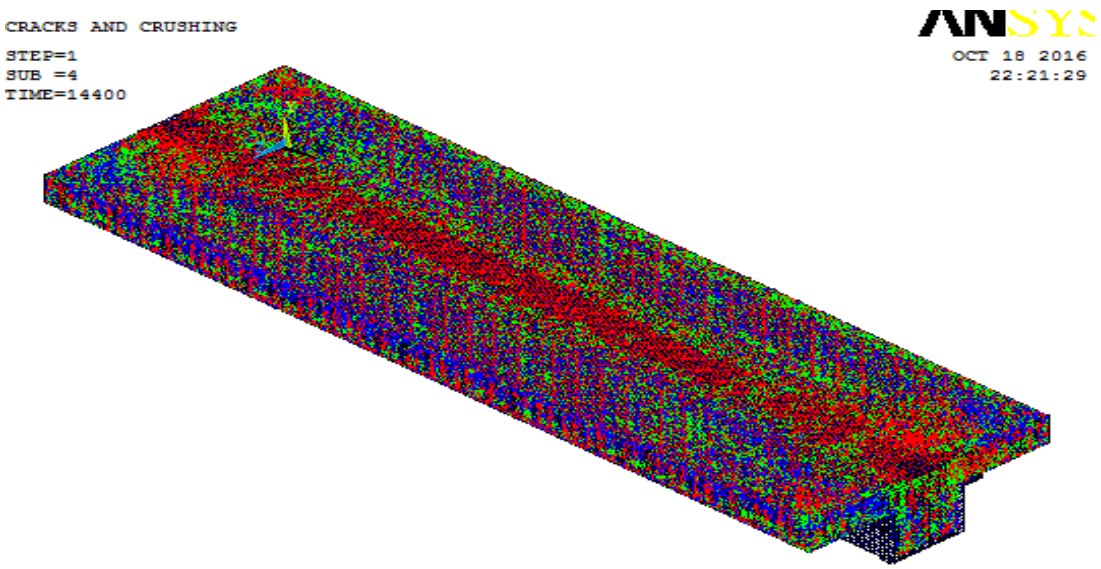

Fig. 10 - Numerical cracking pattern after four hours

CONCLUSION

The paper presents numerical modelling procedure by finite elements that accurately simulate the behaviour of thermally insulated RC beam strengthened in flexure with externally bonded FRP when exposed to standard fire test. Numerical modelling and nonlinear analysis are performed using ANSYS 12.1 [20]. The proposed procedure is verified by comparing the numerical results with experimental results in the published literature. Based on the obtained numerical results, the following conclusions can be drawn:

1. The numerical results of the adopted approach are in good agreement with the published experimental results regarding mid-span deflection and temperature distribution within the cross-section throughout the elevated temperature time history.
2. The proposed model gives more accurate representation for mid-span deflection compared with published numerical results due to using shell elements for FRP, proper representation of the constituent materials used and the refined meshing used in the present model.
3. The presented model managed to predict accurately the full fields of temperatures and deflection in CFRP-strengthened insulated T-beams exposed to underside fire scenario.
4. Numerical results indicate that the mid-span deflection increases nonlinearly throughout the fire exposure time. This is due to the increase in the total strain on the tension side of the beams and due to concrete cracking.
5. The developed finite element model provides reliable coupled thermal-structural results and provides useful information on the fire resistance of insulated strengthened structural member.
6. The developed numerical procedure thereby provides an economic tool to check and design fire protection layers for FRP-strengthened RC beams.

REFERENCES

[1] Bakis, C.E., Bank, L.C., Brown, V.L, Cosenza, Davalos, J.F., Lesko, J.J, Machida, A., Rizkalla, S.H., and Triantafillou, T.C., “Fiber-reinforced polymer composites for construction—state-of-the-art review”, Proceedings of Journal of Composites for Construction, 6 (2002) 73 – 87.

[2] Yu, B., and Kodur, V.K.R., "Effect of temperature on strength and stiffness properties of near-surface mounted FRP reinforcement", Composites Part B: Eng. 58 (2014) 510-517.
[3] Firmo, J.P., Pitta, D, Correia, J.R., Tiago, C., and Arruda, M.R.T., "Experimental characterization of the bond between externally bonded reinforcement (EBR) CFRP strips and concrete at elevated temperatures", Cement Concrete Composites,60 (2015) 44-54.
[4] American Concrete Institute (ACI). ACI 440.2R-08: “Guide for the design and construction of externally bonded FRP systems for strengthening concrete structures”, ACI Committee 440, Farmington Hills, MI, USA, 2008.
[5] ECP Committee 208, ECP 208-05: “Egyptian code of practice for the use of fiber reinforced polymer in the construction field”, ECP Committee 208, Ministry of Housing and Urban Communities, Egypt, 2005.
[6] Blontrock, H., Taerwe, L., and Vandevelde, P. “Fire tests on concrete beams strengthened with fiber composite laminate”, Third Ph.D. Symposium, Vienna, Austria, (2000), 10 pp.
[7] Williams, B., Kodur, V.K.R., Green, M.F., and Bisby, L.A., "Fire endurance of fiber-reinforced polymer strengthened concrete T-beams", ACI Structural Journal, 105(1) (2008) 60-67.
[8] Klamer, E.L., Hordijk, D.A. and Hermes, M.C.J., “The influence of temperature on RC beams strengthened with externally bonded CFRP reinforcement”, Heron, 53(3) (2008)157–185.
[9] Zhu, H., Wu, G., Zhang, L., Zhang, J., and Hui, D., "Experimental study on the fire resistance of RC beams strengthened with near-surface-mounted high-Tg BFRP bars", Composites Part B: Eng., 60 (2014) 680-687.
[10] Firmo, J.P., and Correia, J.R., "Fire behaviour of thermally insulated RC beams strengthened with EBR-CFRP strips: experimental study", Composite Structures,122 (2015) 144-154.
[11] Salama, A.E., Ghanem, G.M. Abd-Elnaby, S.F., El-Hefnawy, A.A., and Abd-Elghaffar, M., “Behavior of thermally protected RC beams strengthened with CFRP under dual effect of elevated temperature and loading”, HBRC Journal, 8(1) (2012) 26–35.
[12] Kamal, O.A., Hamdy, G.A., and Abou-Atteya, M.A., “Efficiency of coating layers used for thermal protection of FRP strengthened beams”, HBRC Journal, 10 (2014) 183–190.
[13] Eurocode 2. EN 1992-1-2: Design of concrete structures. Part 1-2: General rules-Structural fire design, European Committee for Standardization, Brussels, Belgium, 2004.
[14] Williams, B., Kodur, V.K.R., Green, M.F., and Bisby, L., ”Fire endurance of fiber-reinforced polymer strengthened concrete T-beams, J. ACI Struct; 105(1) (2008) 60–67.
[15] American Society for Testing and Materials (ASTM). ASTM E119: Standard Test Methods for Fire Tests of Building Construction and Materials, West Conshohocken, PA, USA, 2007.
[16] Gao, W.Y., Dai, J.G., Teng, J.G., and Chen, G.M., "Finite element modeling of reinforced concrete beams exposed to fire", Engineering Structures, 52 (2013) 488-501.
[17] Dai, J., Gao, W., and Teng, J., "Finite element modeling of insulated FRP-strengthened RC beams exposed to fire", Journal of Composites in Construction, 19(2) (2015)1-15.
[18] Arruda, M.R.T., Firmo, J.P., Correia, J.R., and Tiago, C., "Numerical modelling of the bond between concrete and CFRP laminates at elevated temperatures", Engineering Structures, 110 (2016) 233–243.
[19] Hawileh, R., A., Naser, M., Zaidan, W., and Rasheed, H. A., “Modeling of insulated CFRP strengthened reinforced concrete T-beam exposed to fire”, Eng. Struct., 31 (12) (2009), pp. 3072–3079.
[20] ANSYS. Finite Element Computer Code. Version 12.1.0. ANSYS Inc., Canonsburg, PA, 2009.
[21] Harmathy, T.Z., “Fire Safety Design and Concrete, Concrete Design and Construction Series”, Longman, UK, 1993.

[22] Eurocode 3. EN 1993-1-2: Design of steel structures. Part 1-2: General rules- Structural fire design, European Committee for Standardization, Brussels, Belgium, 2005.
[23] Griffis, C. A., Masmura, R.A., and Chang, C.I., “Thermal response of graphite-epoxy composite subjected to rapid heating”, Journal of Composite Materials., Vol. 15 (1981), pp. 427-442.
[24] Cramer, S.M., Friday, O.M., White, R.H., and Sriprutkiat, G., “Mechanical properties of gypsum board at elevated temperatures”, Fire and Materials (2003) 33–42.
[25] Park, S. H., Manzello, S., L., Bentz, D., P., and Mizukami, T., “Determining thermal properties of gypsum board at elevated temperatures”, Fire and Materials, (2009), pp. 237-250.
[26] Willam, K.J. and Warnke, E.D., “Constitutive model for the triaxial behavior of concrete”, Proceedings of international association for bridge and structural engineering”, ISMES. 1975. Bergamo, Italy, 1975, pp. 1–30.